



Low Serum Uric Acid Levels Promote Hypertensive Intracerebral Hemorrhage by Disrupting the Smooth Muscle Cell-Elastin Contractile Unit and Upregulating the Erk1/2-MMP Axis

Ning Xiao¹ · Tian-long Liu¹ · Hao Li¹ · Hao-chen Xu¹ · Jing Ge¹ · Hong-yan Wen¹ · Cong-xia Bai¹ · Li Song¹ · Ying-ying Sun¹ · Yin-hui Zhang¹ · Ru-tai Hui¹ · Wei-hua Song¹ · Jing-zhou Chen¹

Received: 16 July 2019 / Revised: 7 February 2020 / Accepted: 12 February 2020 / Published online: 22 April 2020
© Springer Science+Business Media, LLC, part of Springer Nature 2020

Abstract

Intracerebral hemorrhage (ICH) is a catastrophic stroke with high mortality, and the mechanism underlying ICH is largely unknown. Previous studies have shown that high serum uric acid (SUA) levels are an independent risk factor for hypertension, cardiovascular disease (CVD), and ischemic stroke. However, our metabolomics data showed that SUA levels were lower in recurrent intracerebral hemorrhage (R-ICH) patients than in ICH patients, indicating that lower SUA might contribute to ICH. In this study, we confirmed the association between low SUA levels and the risk for recurrence of ICH and for cardiac-cerebral vascular mortality in hypertensive patients. To determine the mechanism by which low SUA effects ICH pathogenesis, we developed the first low SUA mouse model and conducted transcriptome profiling of the cerebrovasculature of ICH mice. When combining these assessments with pathological morphology, we found that low SUA levels led to ICH in mice with angiotensin II (Ang II)-induced hypertension and aggravated the pathological progression of ICH. In vitro, our results showed that p-Erk1/2-MMP axis were involved in the low UA-induce degradation of elastin, and that physiological concentrations of UA and p-Erk1/2-specific inhibitor exerted a protective role. This is the first report describing to the disruption of the smooth muscle cell (SMC)-elastin contractile units in ICH. Most importantly, we revealed that the upregulation of the p-Erk1/2-MMP axis, which promotes the degradation of elastin, plays a vital role in mediating low SUA levels to exacerbate cerebrovascular rupture during the ICH process.

Keywords Intracerebral hemorrhage · Uric acid · Erk1/2 · MMPs

Introduction

Intracerebral hemorrhage (ICH) is a catastrophic type of stroke with high mortality and morbidity and a substantial risk of recurrence in adults [1]. Hypertension is the most important risk factor for hemorrhagic stroke [2, 3]; however,

hypertensive people do not always develop ICH. According to a 12-year follow-up study, 0.5% of hypertensive patients developed ICH, and antihypertensive treatment may help reduce the risk of cerebral hemorrhage, although some patients with this treatment still develop ICH [4]. Taken together, these data suggest that there may be other risk factors that combined with hypertension result in ICH.

Uric acid (UA), the final product of purine degradation, has emerged as a biomarker for a predisposition toward metabolic syndrome, hypertension, diabetes, and cardiovascular and renal disorders [5–7]. Several studies have shown that there is an association between high serum uric acid (SUA) levels and the risk of hypertension, cardiovascular disease (CVD), and ischemic stroke [8, 9]. Our metabolomics data showed that SUA levels were lower in recurrent ICH (R-ICH) patients than in ICH patients. We also found that the hypertensive ICH group had significantly lower SUA levels; there were no significant differences between the thrombosis and lacunar

Electronic supplementary material The online version of this article (<https://doi.org/10.1007/s12975-020-00791-3>) contains supplementary material, which is available to authorized users.

✉ Wei-hua Song
songweihua926@163.com

✉ Jing-zhou Chen
chendragon1976@aliyun.com

¹ State Key Laboratory of Cardiovascular Disease, Fuwai Hospital, Chinese Academy of Medical Science and Peking Union Medical College, Beijing 100037, China

groups. These data suggest that low SUA levels may be a risk factor for ICH.

In addition, although ICH is a devastating disease, its molecular mechanisms and pathology remain poorly understood. Donald D and colleagues described the first mouse model of spontaneous hemorrhagic stroke (8 months old), in which ICH was induced by angiotensin II (Ang II) and N^ω-nitro-L-arginine methyl ester (L-NAME), and explored the ICH mechanisms in mice with acute and chronic hypertension [10–12]. Their data suggested that oxidative stress and MMPs contribute to spontaneous ICH. However, using the same mouse model to induce hypertension in young mice (16 weeks), Anja et al. observed altered cerebrovascular structures but only sporadic microbleeding and no severe ICH [13]. In a recent study, miconazole was shown to protect blood vessels from matrix metalloproteinase-9 (MMP-9)-dependent rupture and hemorrhage in zebrafish [14].

Currently, there is no consensus regarding the linkage between low SUA and ICH. In addition, to the best of our knowledge, no systematic studies have evaluated the molecular basis of ICH. Therefore, the present study was performed to investigate the association between low SUA levels and the risk of ICH. Furthermore, we intend to characterize the cellular and molecular mechanisms involved in the development of ICH in individuals with low SUA levels to shed light on the role of SUA in the diagnosis and therapies for ICH.

Materials and Methods

Sample Population

Patient information in this study was extracted from medical records residing in our team's comprehensive database. We enrolled control subjects and patients with one of the following three subtypes of stroke: cerebral thrombosis (thrombosis), lacunar infarction (lacunar), and hypertensive ICH. The criteria for diagnosis and recruitment were based on neurological examination after computed tomography (CT), magnetic resonance imaging (MRI), or both, as described previously [15]. The end points were recurrence of ICH and death from cardiac-cerebral vascular disease. The details are described in the [Supplementary Materials](#).

Metabolomics Study

We enrolled patients with hypertensive intracerebral hemorrhage (ICH, $n = 53$) and age- and sex-matched patients with recurrent intracerebral hemorrhage (R-ICH, $n = 62$), who were obtained from the cohort mentioned above. Patients or their caregivers provided informed consent.

We detected plasma metabolites by ultra-performance liquid chromatography coupled with electrospray ionization/

quadrupole-time-of-flight mass spectrometry (UHPLC-Q/TOF-MS) and analyzed the data with multivariate statistics to compare outcomes among the groups.

Clinical Outcomes

We recruited 1669 control subjects and 1469 patients and compared SUA levels among the three subtypes of stroke and healthy controls. Among the 1469 cases, 667 were diagnosed with thrombosis, 451 were diagnosed with lacunae, and 351 were diagnosed with ICH.

To examine the associations between SUA levels and either hypertensive R-ICH or cardiac-cerebral vascular mortality, the study participants were stratified by SUA levels, and ICH patients over 60 years old were categorized into 2 groups: a low UA group ($\leq 236 \mu\text{mol/L}$) and a high UA group ($> 236 \mu\text{mol/L}$). Kaplan-Meier plots were created to estimate the effects of UA levels on the risk of hypertensive R-ICH and cardiac-cerebral vascular disease mortality after a median 4.5 years of follow-up. The results were compared by the log-rank test.

Low Serum Uric Acid Mouse Model

Commercially available 8-month-old male C57BL/6 mice were purchased from the National Resource Center of Model Mice (Nanjing, China). All animals were housed in a conventional housing facility under a standard 12:12-h light-dark cycle.

After adaptive feeding for 1 week, the mice were randomly divided into 4 experimental groups: control ($n = 5$), allopurinol ($n = 5$), benzbromarone ($n = 5$), and allopurinol and benzbromarone (A + B, $n = 5$). To produce the low UA model, allopurinol (20 mg/kg per day; Shimaotianjie, China) and/or benzbromarone (20 mg/kg per day; Excella GmbH, Germany) were dissolved in sterile saline and administered by oral gavage. Thirty days later, the mice were anesthetized, and blood samples were collected. We measured SUA levels in accordance with the manufacturer instructions (Abcam, USA).

Spontaneous Intracerebral Hemorrhage Model

Spontaneous ICH models were induced as described previously [11]. Mice were randomly divided into 5 experimental groups: vehicle (Veh, $n = 30$), Ang II (A, $n = 30$), Ang II and L-NAME (AL, $n = 30$), Ang II and low UA (A + LU, $n = 30$), and Ang II and L-NAME and low UA (AL + LU, $n = 30$). Mice in the Veh and A groups were infused with Ang II (1000 ng/kg per min; Sigma-Aldrich, USA) or an equivalent volume of saline, respectively, via an osmotic pump (Durect Corporation, USA). In the AL group, mice were concomitantly administered Ang II as described above and L-NAME (100 mg/kg per day; Sigma-Aldrich, USA) in drinking water.

In the two low UA groups (A + LU and AL + LU), allopurinol (20 mg/kg per day) and benzbromarone (20 mg/kg per day) were administered for 30 days, and then the two groups were administered Ang II and/or L-NAME as described above along with continuous allopurinol and benzbromarone administration.

After an initial training period of 7 days, systolic blood pressure (SBP) was measured in conscious mice using tail-cuff plethysmography (LE 5002; Panlab, Cornella, Spain) as described previously [13]. We examined clinical stroke signs by neurologic examinations at least three times per day as described previously [11] and evaluated the incidence of ICH ($n = 20$). At the end of the 28-day treatment period, the animals were anesthetized, and blood samples were collected. The SUA levels were measured in accordance with the manufacturer instructions.

Intracerebral Hemorrhage Assessment by MRI

MRI was performed on a dedicated 7.0-T MR Varian horizontal bore MRI system (Agilent, USA). Briefly, mice were anesthetized with 2% isoflurane in an O₂ mixture (1 L/min). The image protocol comprised T2-weighted imaging with a fast spine echo (FSE) sequence. The parameters used for image acquisition in the mice were as follows: repetition time (TR) = 3500 ms; echo time (TE) = 72.0 ms; thickness = 0.5 mm; acquisition matrix = 256 × 256; and scan time = 16 min. The qualitative evaluation of hemorrhage was performed semi-quantitatively as follows: an investigator blinded to the treatment observed the numbers of hemorrhage points from serially captured MRI photographs. The total number of hemorrhage points in each mouse was calculated in the AL and AL-LU groups ($n = 4$ per group).

RNA Sequencing (RNA-seq)

At the end of the 28-day treatment period, the animals were anesthetized. After removing meningeal vessels, we homogenized the brain tissues with a Dounce homogenizer and isolated cerebral vessels as described previously [16, 17]. Then, total RNA was isolated from the cerebrovascular segment using an RNeasy Mini Kit (Qiagen, Germany) according to the manufacturer recommendations. TruSeq Stranded Total RNA with a Ribo-Zero Human Kit (Illumina, USA) was used to obtain sequencing libraries. Ninety million 2 × 100-bp paired end reads were sequenced on an Illumina HiSeq 2500 Sequencing system for each library ($n = 5$ in the Veh, A and AL groups; $n = 4$ in the A + LU and AL + LU groups). Analysis of differential transcript expression was performed with the Cuffdiff program. The details of this analysis are described in the [Supplementary Materials](#).

Bioinformatics Analysis

To dissect the relationships among the groups under the given conditions based on the molecular profiles, we applied multi-dimensional scaling (MDS) analysis to the distance matrix and placed all the samples into a 2-dimensional Euclidian space using R software (<https://www.r-project.org/>). Ingenuity Pathway Analysis (Ingenuity Systems, USA) was applied to obtain additional insights based on a manually curated database.

Histology and Immunofluorescence

Mice were euthanized with an overdose of 3% chloral hydrate (i.p.). The brains were harvested, fixed in 4% paraformaldehyde (PFA) overnight at 4 °C, paraffin-embedded, and then dehydrated using a graded ethanol series and vitrification by xylene. Serial horizontal sections (4 μm) were sliced with a microtome (Leica Biosystems). Hematoxylin-eosin (HE) staining was applied to observe hemorrhages. Images were captured on a Leica DMI-4000B digital microscope.

For immunofluorescent staining, horizontal brain sections (4 μm) were incubated with the following primary antibodies: anti- α -smooth muscle actin (α -SMA, Abcam, 1:300), anti-elastin (Abcam, 1:50), and anti-phospho-p44/42 MAPK (p-Erk1/2, CST, 1:100). After several washes, the sections were incubated with secondary antibodies (Alexa Fluor-conjugated goat anti-mouse or anti-rabbit; Life Technologies) at room temperature for 1 h. The sections were then mounted in aqueous DAPI-containing medium (Abcam). Immunostaining images were captured under a confocal microscope (Leica) with microscope image-acquisition software.

Qualitative evaluation of elastin filament integrity was performed by an observer blinded to the treatment conditions on digital images by semiquantitative grading ($n = 5$) as previously reported [18, 19]. We analyzed the cerebral vessels mainly from corpus striatum. The diameters of the cerebral vessels analyzed in our study were from 10 to 50 μm, which in accordance with the levels of LSAs, especially when observed by immunofluorescence [20].

In Situ MMP Activation Detection and Immunofluorescence

To assess in situ gelatinolytic activity, frozen coronal sections (20 μm) were incubated with DQ gelatin conjugate at 37 °C for 2 h with a commercially available kit (EnzCheck Gelatinase Assay Kit; Invitrogen). Then, the sections were washed and labeled with the following primary antibodies: anti- α -SMA (Abcam, 1:300). Confocal images were captured using a confocal microscope (Leica) with microscope image-acquisition software. MMP expression was presented as the percentage of the MMP-positive area covering the α -SMA-

positive area in the vessels. Quantitative measurements of the coverage were conducted with *AngioTool* software, and representative images of each group were collected in 5 mice.

Cell Culture and Experiment

UA Treatment

Primary human brain vascular smooth muscle cells (HBSMCs) were purchased from Shanghai Saily Biological Technology Co., Ltd. According to the manufacturer recommendations, HBSMCs were cultured at 37 °C under 5% CO₂ in DMEM/F-12 medium with 10% fetal bovine serum (FBS) and used for up to five passages. Low concentrations of UA (0.6 mg/dL; Sigma) were freshly prepared, which dissolved in warmed medium and filtered through a 0.22- μ m syringe filter. After the cells were starved for 12 h, the HBSMCs were pretreated with low concentrations of UA (0.6 mg/dL) for up to 24 h. Subsequently, the HBSMCs were exposed to (1) physiological concentrations of UA (6 mg/dL), (2) low concentrations of UA (0.6 mg/dL), and (3) a low concentration UA (0.6 mg/dL) plus specific inhibitors of Erk1/2 phosphorylation (PD98059, 10 μ M; Sigma) in Western blot, in situ MMP activation detection, and elastin expression arrays. Experiment flow chart was shown in Fig. S4a.

Western Blot Analysis

Cells were lysed in ice-cold RIPA buffer containing phosphatase inhibitor and protease inhibitor cocktail (Roche). Protein content was quantified by a BCA protein assay kit (Thermo Fisher Scientific). Samples (20 μ g) were subjected to sodium dodecyl sulfate-polyacrylamide gel electrophoresis (SDS-PAGE) and transferred to nitrocellulose membranes (Promega) and blocked with 5% nonfat dry milk in Tris-buffered saline containing 0.05% Tween 20. Membranes were incubated overnight with primary antibodies respectively: anti-p-Erk1/2 (1:1000, CST), and anti-Total-Erk1/2 (T-Erk1/2, 1:1000, CST). The specific bands were visualized using secondary anti-rabbit antibody (1:5000, Abcam), and enhanced chemiluminescence detection kit (Thermo Fisher Scientific). The intensity of protein bands was measured with ImageJ software.

In Situ MMP Activation Detection and Elastin Expression Array

To detect in situ MMP activation and elastin expression, HBSMCs were seeded at a density of 5000 cells per well into a 96-well CellCarrier™ microtiter plate (PerkinElmer). After the cells were starved, then were pretreated with a low level of UA and exposed to different treatments in phenol red-free medium; they were then fixed in 4% PFA, permeabilized with 0.2% Triton X-100, and incubated with DQ gelatin conjugate

at 37 °C for 2 h using a commercial kit (EnzCheck Gelatinase Assay Kit; Invitrogen). Subsequently, the cells were labeled with the following primary antibodies: anti- α -SMA (Abcam, 1:300) and elastin (Abcam, 1:120), followed by an AlexaFluor®568 and 647 secondary antibody (1:300, Life Technologies). Nuclei were stained using a 10 μ M Hoechst 33342 dye solution (Invitrogen). The plates were then imaged on an Operetta® High Content Screening system (PerkinElmer) in widefield fluorescence mode using a \times 40 high water objective. Five random fields per well and 4 replicate wells were imaged and analyzed. The approach for image analysis in the Harmony® software was based on counting nuclei (Hoechst channel), followed by a per cell fluorescence intensity analysis (MMP channel and Elastin channel, respectively).

Statistical Analysis

Data are expressed as the mean \pm SDs. Comparisons between two groups were analyzed by Student's *t* test, whereas comparisons among 3 or more groups were conducted by ANOVA with Bonferroni multiple comparisons. All data were analyzed using GraphPad Prism 7.0 software and SPSS 19.0 software. A *P* value < 0.05 was considered statistically significant.

Results

Low SUA Increased the Risk for R-ICH and Cardiac-Cerebral Vascular Mortality

A total of 3138 subjects were enrolled in this study, including 1669 control subjects and 1469 stroke patients (667 in the thrombosis group, 451 in the lacunar group, and 351 in the hypertensive ICH group), who were selected for chi-square analysis SUA level differences. The SUA levels in the different stroke subtypes are shown in Table 1. Compared with the control group, the hypertensive ICH group had significantly lower SUA levels (*P* < 0.01), but the thrombosis and lacunar groups showed no significant differences.

Table 1 The serum UA level in different subtypes of stroke

Group	Subjects (<i>n</i>)	Uric acid (μ mol/L)	<i>P</i> value*
Controls	1669	269.10 (\pm 72.45)	1.0
Stroke	1469	263.74 (\pm 86.79)	0.06
Thrombosis	667	266.24 (\pm 85.10)	0.45
Lacunar	451	272.06 (\pm 82.63)	0.45
Hypertensive ICH	351	248.30 \pm 93.23)	9.60 \times 10 ⁻⁵ Δ

*Student's *t* test vs controls. Δ *P* < 0.01 vs control

We applied untargeted metabolomics to analyze the differences in plasma metabolites between ICH and R-ICH. The metabolic profiles clearly distinguished ICH patients and R-ICH patients, and orthogonal projection to latent structure-discriminant analysis (OPLS-DA) showed that there were differences in the profile of small molecular metabolite profiles between the two groups (Fig. 1a). SUA levels were significantly lower in the R-ICH group than in the ICH group, ($P < 0.05$) (Fig. 1b).

Over a median follow-up of 4.5 years in ICH patients over 60 years old, our data indicate that low SUA levels ($\leq 236 \mu\text{mol/L}$) were associated with a higher risk of R-ICH ($P = 0.011$, HR = 3.23, 95% CI 1.20 to 8.71; Fig. 1c). We also found that low SUA levels ($\leq 236 \mu\text{mol/L}$) carried a higher risk for mortality by cardiac-cerebral vascular disease ($P = 0.008$, HR = 3.25, 95% CI 1.37 to 7.7; Fig. 1d). Taken together, the results of our population-based study support the notion that there is an association between low SUA levels and an

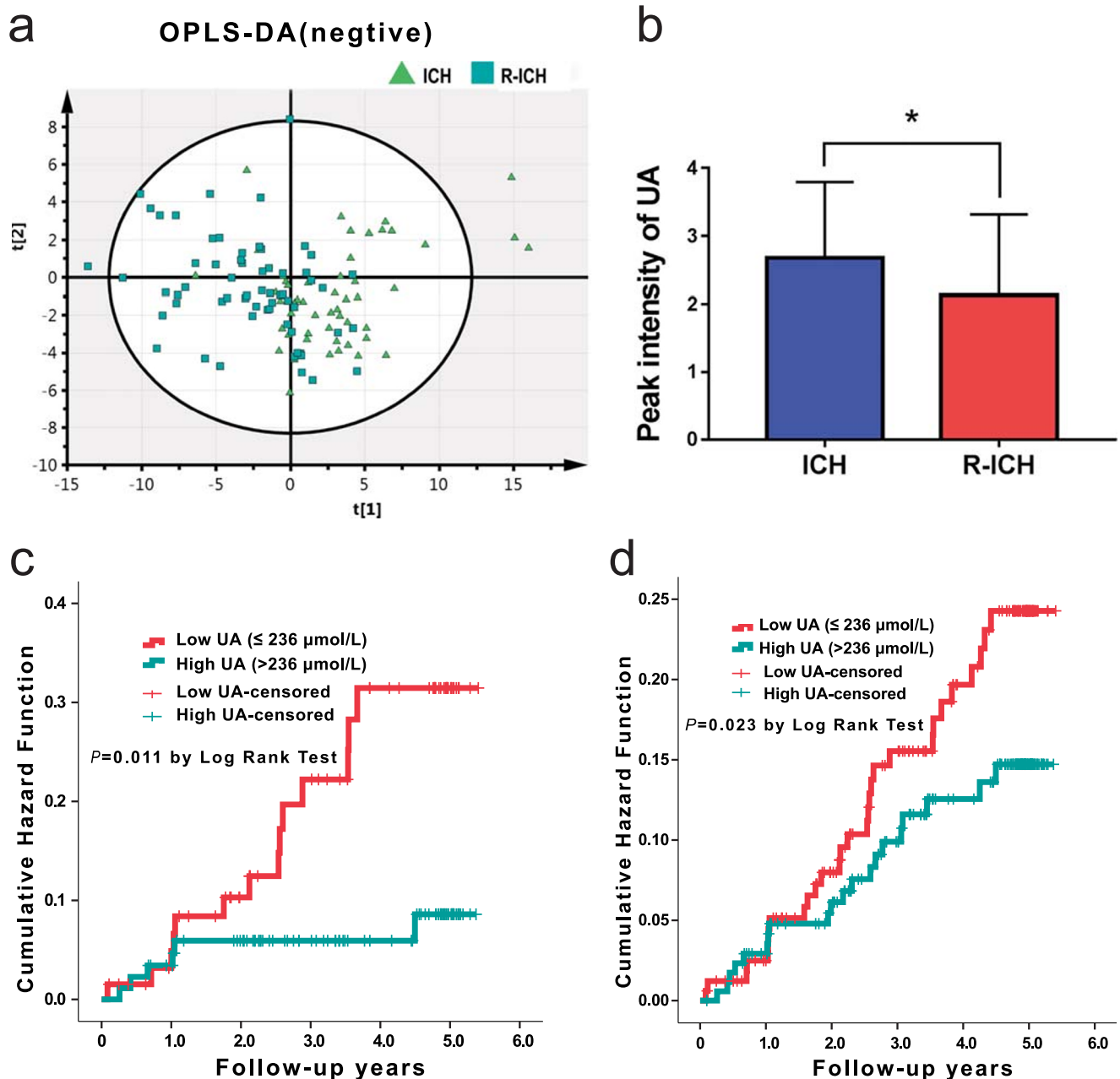


Fig. 1 Population results from human subjects. **a** Score scatterplot of metabolites in the ICH and R-ICH groups by orthogonal projections to latent structures discriminant analysis (OPLS-DA). **b** Metabolomics results showed that UA was significantly lower in the R-ICH group

than in the ICH group. Kaplan-Meier analysis illustrating **c** survival of R-ICH and **d** cardiac-cerebral vascular mortality in subjects stratified into two groups according to UA level after a median of 4.5-year follow-up. * $p < 0.05$

increased risk of R-ICH and cardiac-cerebral vascular mortality in ICH patients over 60 years old.

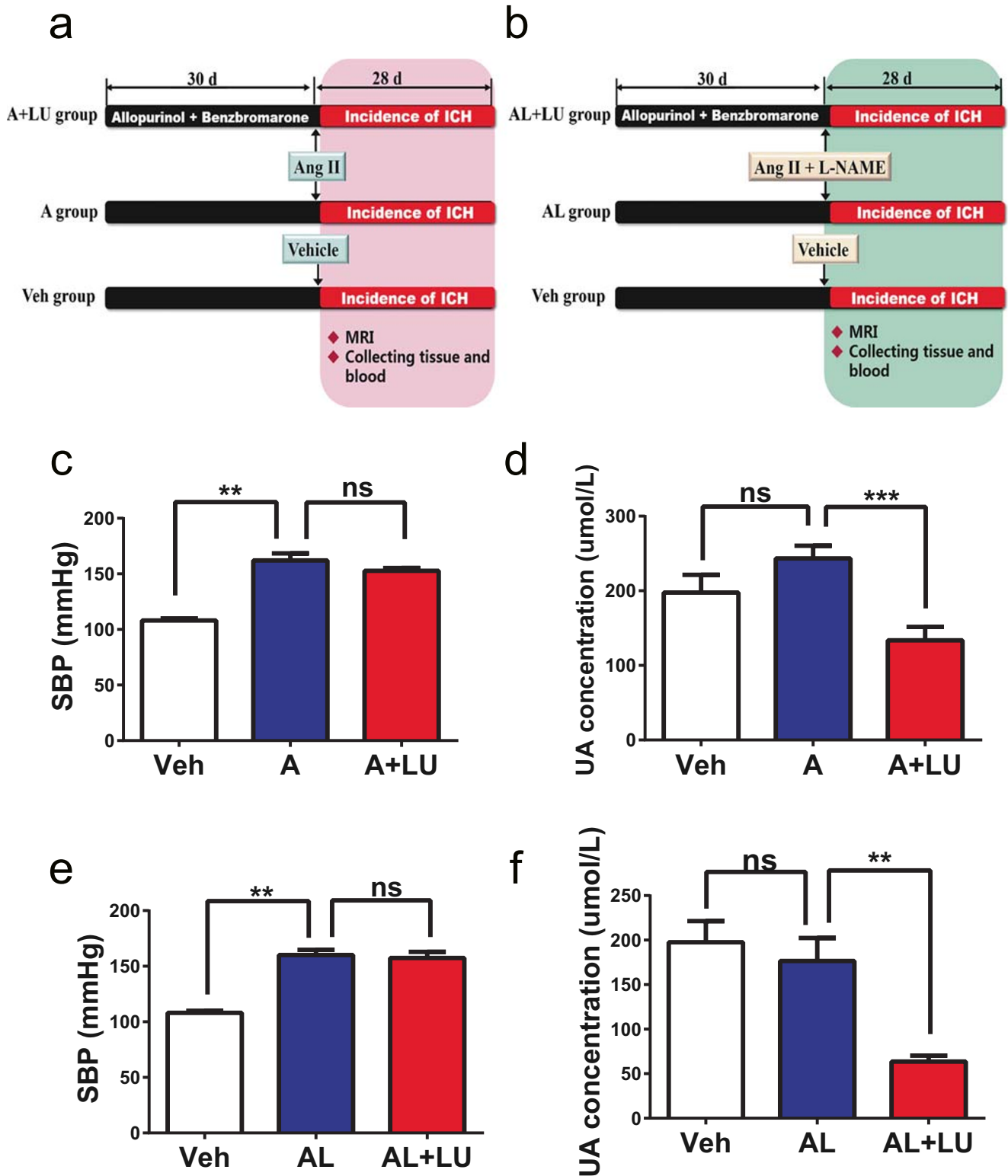


Fig. 2 Low uric acid model in hypertensive mice. **a, b** Experiment flow chart. **c, e** SBP in the different groups as measured by the tail-cuff method ($n = 10$). **d, f** Serum UA concentration in the different groups ($n = 8$). $**p < 0.01$; ns, not significant

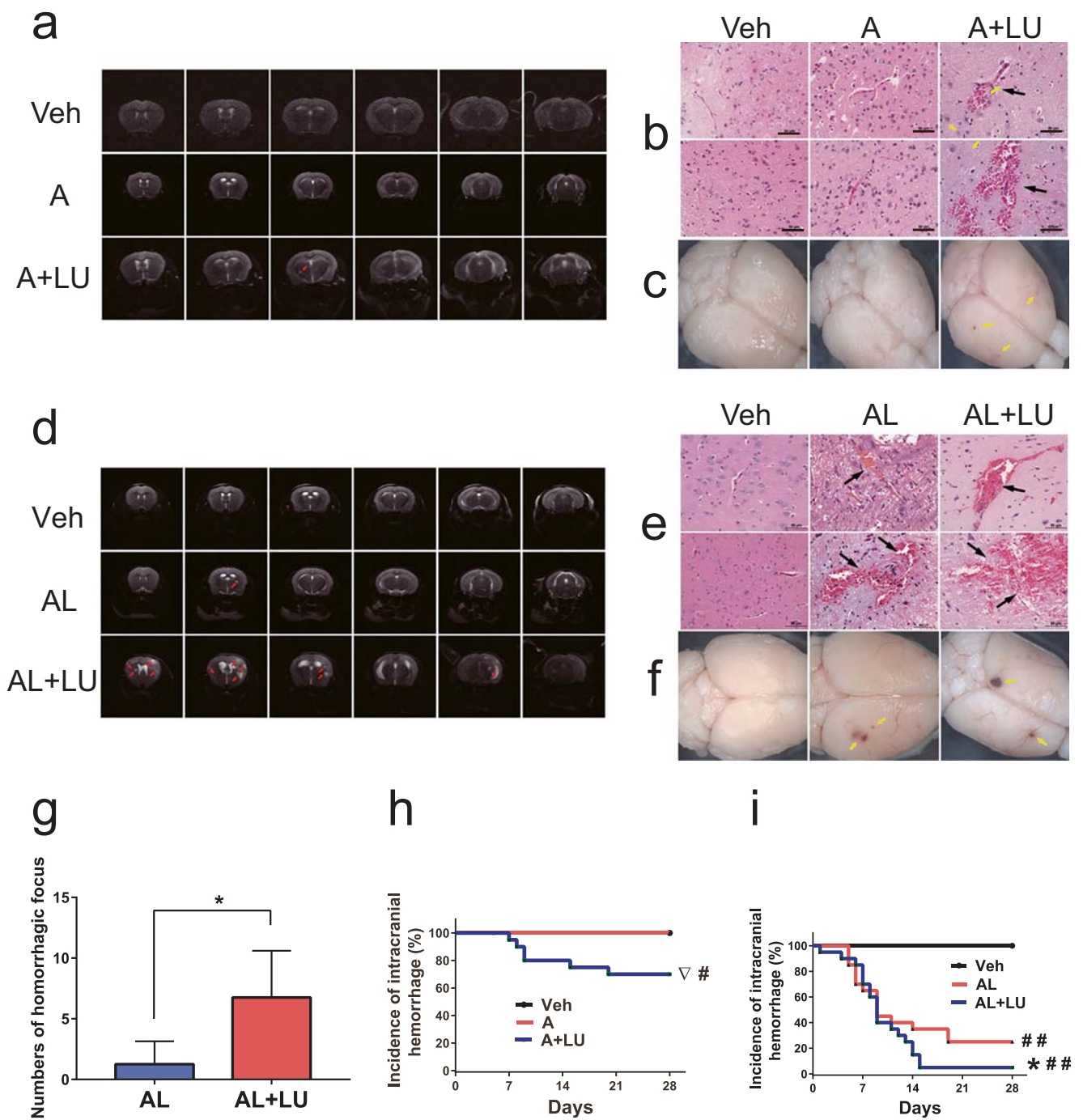


Fig. 3 Low uric acid promoted ICH in hypertensive mice. **a, d** T2-weighted images of brain from the different groups were obtained by 7-T MRI. Red arrows highlighting increased signal intensity indicate hemorrhage in the brain. **b, e** Representative images of HE staining in the different groups. Black arrows indicate hemorrhage (scale bars, 50 μ m). **c, f** The brain morphology of each group. Yellow arrows

indicate hemorrhage. **g** MRI scanning showed more hemorrhagic foci in the AL+LU group than in the AL group ($n = 4$, $p < 0.05$). **h, i** Kaplan-Meier plot of the signs of stroke ($n = 20$). In **g** $*p < 0.05$; in **h** and **i** $\Delta p < 0.05$ vs the A group, $\#p < 0.05$ and $\#\#p < 0.01$ vs the Veh group; $*p < 0.05$ vs the AL group

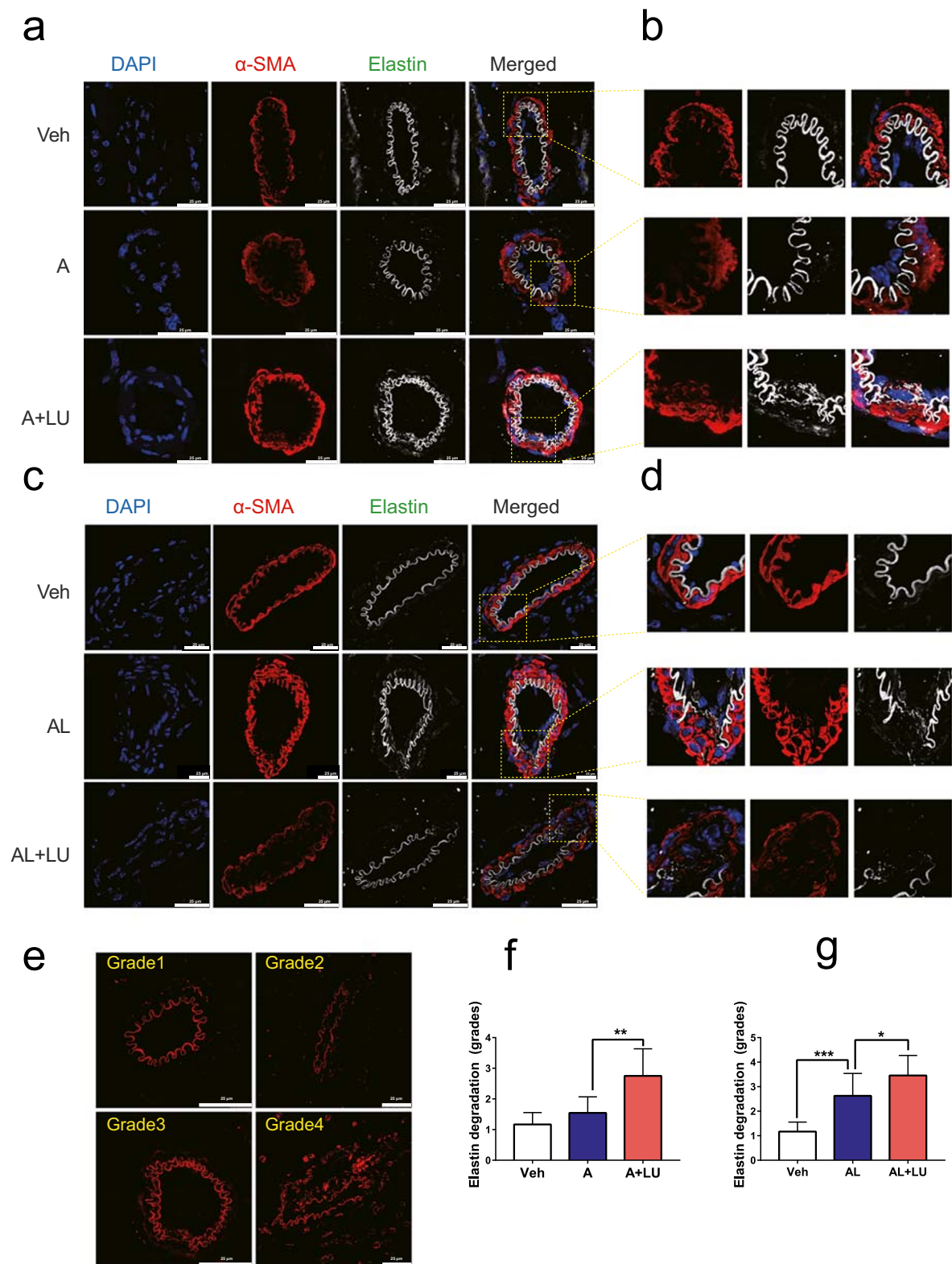


Fig. 4 Low uric acid accelerated the disruption of SMC-elastin contractile units in hypertensive mice. **a, c** Representative images of brain sections showing cerebral vessel staining of each group; DAPI in blue, α-SMA in red, and elastin in gray. **b, d** Insets show an SMC-elastin contractile unit at high magnification. **e** Cerebral vascular elastin

degradation was graded on a scale of 1 to 4. Examples of grading are shown, and the method is detailed in the Materials and Methods. **f, g** The level of elastin degradation (grades 1–4) in the different groups. * $p < 0.05$, ** $p < 0.01$; ns, not significant. (Scales bar are shown in the image)

Low SUA Led to the Development of ICH and Accelerated ICH Progression in Hypertensive Mice

Because there was no low UA model, we first established a low UA mouse model using allopurinol (which inhibits UA production) and benzbromarone (which promotes UA excretion). Compared with the control group, in the group administered these drugs for 30 days, SUA levels were significantly lower (Fig. S1a). HE staining showed that the cerebrovascular structures were intact, and there were no differences between the control group and either the allopurinol or benzbromarone groups. No hemorrhage was observed in any of the LU groups (Fig. S1b).

To explore the association between low SUA levels and ICH, we implemented our LU model in hypertensive mice (Fig. 2a, b). Administration of UA-lowering drugs decreased SUA levels in the A + LU and AL + LU groups (Fig. 2d, f) but had no significant effect on SBP (Fig. 2c, e). Previous studies have reported that the A group showed no ICH phenotype, and we observed the same results. However, in our study, six of the 20 mice in the A + LU group developed signs of hemorrhagic stroke after Ang II infusion. The incidence of ICH was significantly higher in the A + LU group than in the A group (30% vs 0%, $P < 0.05$; Fig. 3h). Hemorrhage was observed in mice in the A + LU group that showed signs of stroke (Fig. 3a–c).

Furthermore, our data showed that in the low SUA groups, ICH progression was significantly faster in the AL + LU group (Fig. 3e, f) than in the AL group. Compared with the Veh group, the AL group (i.e., spontaneous ICH mice) had a significantly higher incidence of ICH (0% vs 65%, $P < 0.01$). The incidence of ICH was significantly higher in the AL + LU group than in the AL group (95% vs 65%, $P < 0.05$, Fig. 3i).

When MRI scans were conducted to detect hemorrhagic lesions in the brains of ICH mice, there were more hemorrhagic foci in the AL + LU group than in the AL group (Fig. 3d, g).

On the one hand, our findings corroborated evidence indicating that low SUA levels contribute to ICH in mice with Ang II–induced hypertension. On the other hand, our results support the notion that a low SUA level is associated with ICH deterioration and an increase in ICH incidence in mice with Ang II– and L-NAME-induced hypertension.

Low SUA Accelerated the Disruption of SMC-Elastin Contractile Units in Hypertensive Mice

The smooth muscle cell (SMC)-elastin contractile unit is the functional and structural unit of the aorta, and the primary pathological changes observed in the rupture of a thoracic aortic aneurysm (TAA) is the disruption of the SMC-elastin contractile unit. As shown in Fig. 4, ICH mice exhibited disruption of SMC-elastin contractile units (Fig. 4a, c) and elastin fragmentation, while in the A and Veh groups, the zigzag

shape of elastin appeared intact, without fragmentation or breakage (Fig. 4b, d). The degree of elastin degradation was higher in the A + LU group than in the A group and more pronounced in the AL + LU group than in the AL group (Fig. 4e–g). These findings indicated that low SUA levels significantly decreased the integrity of the SMC-elastin contractile unit, resulting in cerebrovascular rupture.

Transcriptome Analysis Highlighted the Erk1/2 Pathway

To identify the core transcriptional signature of mice with low UA as it relates to the formation and progression of ICH, we used RNA-seq to analyze the whole transcriptome of the cerebrovasculature in different mouse groups (Fig. 5a). Compared with the Veh group, the A group had 743 differentially expressed genes (DEGs), and the AL group had 2717 DEGs. The data shown in Table 2 demonstrate that compared with Ang II treatment alone (A group), A + LU treatment upregulated 129 genes and downregulated 72 genes, whereas compared with the Ang II and L-NAME alone (AL group), AL + LU treatment resulted in the downregulation of 136 genes and the upregulation of 1123 genes. MDS analysis of all the genes expressed in the 5 sorted groups showed that the greater distances were between the ICH groups (AL, A + LU, and AL + LU groups) and the non-ICH groups (Veh and A groups). The distance between the non-ICH groups and the AL + LU group was the largest, while the A + LU and AL groups were very similar (Fig. 5b).

The top 1 network operating in the A + LU group vs the Veh group is shown in Fig. 5c. Among the genes in this network, brain-derived neurotrophic factor (BDNF) and extracellular regulated protein kinases 1 and 2 (Erk1/2) are the hub genes. Although there was no significant difference between the A + LU group and the A group, Erk1/2 had the highest centrality. We further found that Erk1/2 and MAPK1 (Erk2) were also involved in the top causal networks and showed a high centrality between the AL + LU group and the Veh group based on IPA ($P = 7.9E-26$, Fig. 5d). Based on these results, Erk1/2 was selected for further validation.

Low SUA Levels Promoted ICH by Increasing the Activation of the Erk1/2-MMP Axis

To confirm the role of Erk1/2 in promoting ICH, we examined the expression of phosphorylated Erk1/2 (p-Erk1/2) in the cerebrovasculature in situ using immunofluorescence. The results showed faint p-Erk1/2 staining in the Veh group, positive staining on the intima in the A group, and strong expression in the media and periphery in the A + LU group (Fig. 6a, b). Although there was no significant difference in the staining intensity of the media, p-Erk1/2-positive staining of the intima

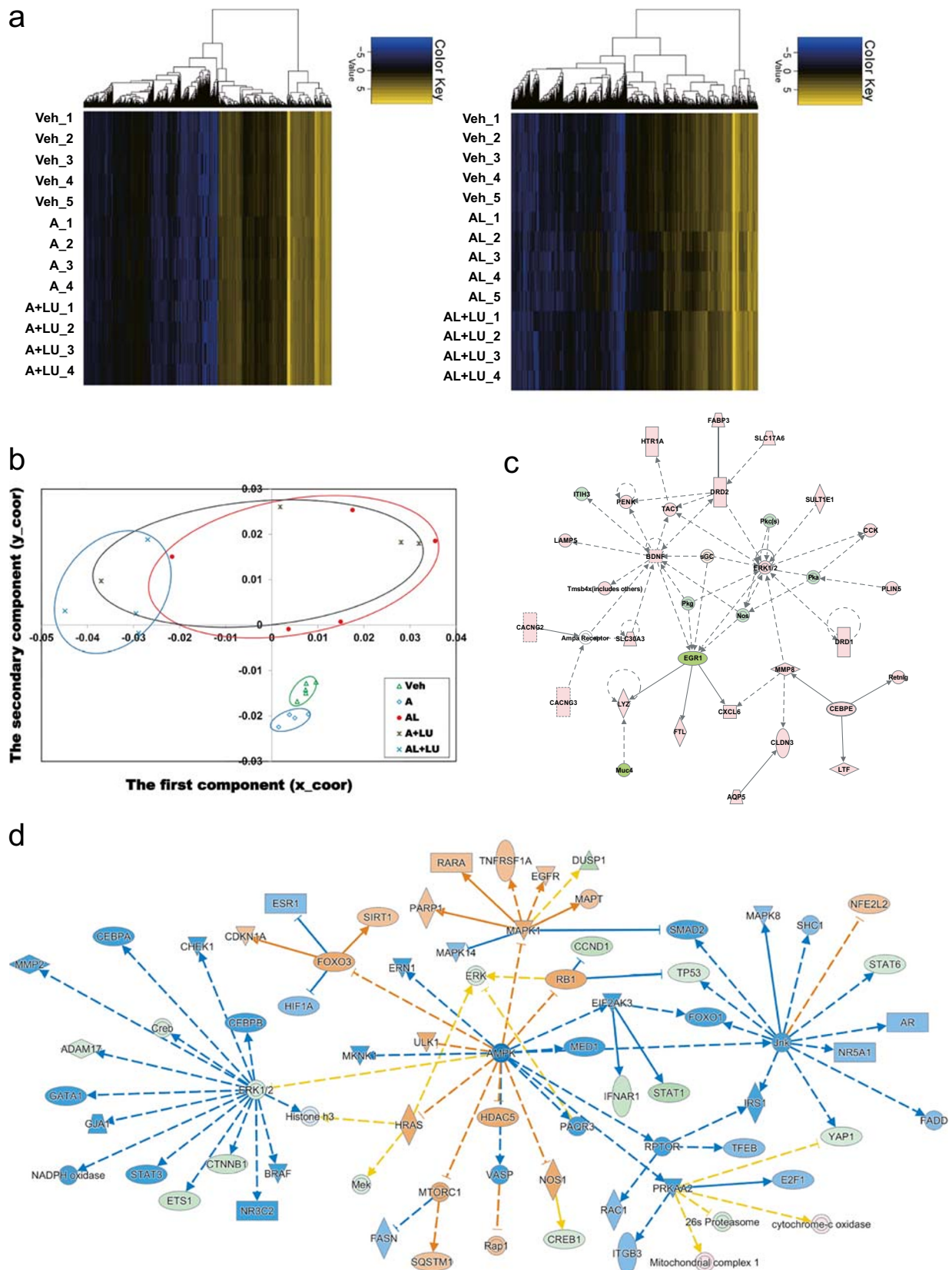


Fig. 5 Analysis based on RNA-seq data. **a** Expression heat map of different groups (yellow, high; blue, low). **b** MDS plot showing clustering of the similarity matrix for the 5 groups. **c** The top network

operative among genes in the A+LU group versus those in A group as assessed by Ingenuity Pathway Analysis. **d** Ingenuity Pathway Analysis of the top causal network between the AL+LU and AL groups

Table 2 Differentially expressed genes (DEGs) across five groups

DEGs	A vs Veh	A + LU vs A	AL vs Veh	AL + LU vs AL
Upregulated	311	129	1781	1123
Downregulated	432	72	936	136
Total	743	201	2717	1259

and periphery was more intense in the AL + LU group than in the AL group (Fig. 6c, d).

Previous studies have revealed a strong correlation between Erk1/2 and MMP9 in aortic aneurysms and brain hemorrhages in zebrafish [14]. We next examined whether MMP activity was also elevated in the ICH groups. Immunofluorescence combined with in situ zymography suggested that in situ MMP activity colocalized with α -SMA (Fig. 7a, c). In the A group, the cerebrovascular exhibited low overlap between MMPs and α -SMA⁺ coverage; however, the A + LU group showed significantly greater overlap than was observed in the A group (Fig. 7b). There was no significant difference between the AL and AL + LU groups regarding the overlap in coverage of MMP- α -SMA⁺ (Fig. 7d). Furthermore, the 3D images exhibited a critical impairment of the cerebrovascular structure in the ICH groups (Fig. S3). Mice in the Veh group presented dense and thick collagen fibers, while the mice in the A group maintained relatively dispersed, thin collagen fibers. In the ICH groups, collagens were severely fragmented and disorganized, especially in the AL + LU group.

Low Concentration UA Increased p-Erk1/2-MMP Activity and Elastin Degradation In Vitro

To further confirm the relationship between low UA levels, Erk phosphorylation, and elastin damage, we examined whether low concentration UA (0.6 mg/dL) exposure increased the phosphorylation of Erk1/2, MMP activity, and degraded elastin expression in HBSMCs. Our data showed that after pretreatment with 0.6 mg/dL UA for 24 h, p-Erk1/2 phosphorylation was observed from 15 to 240 min, whereas physiological concentrations of UA (6 mg/dL) and PD98059 (p-Erk1/2 phosphorylation inhibitor) decreased phospho-Erk1/2 levels (Fig. S4b and 4c). At 240 min, compared with 6 mg/dL UA, 0.6 mg/dL UA significantly increased phospho-Erk1/2 ($P < 0.001$, Fig. 8a, b), MMP activity ($P < 0.001$, Fig. 8d), and degraded elastin expression ($P < 0.001$, Fig. 8d). These data demonstrate that low UA levels induced activation of MMPs via Erk1/2 signaling pathway and partially inhibited by physiological concentration of UA (6 mg/dL). This was confirmed by our finding that the p-Erk1/2 phosphorylation inhibitor PD98059 (0.6 mg/dL + PD98059 group) decreased low UA-induced MMP activity, in part by dephosphorylating Erk1/2 (Fig. 8).

These findings indicate that p-Erk1/2-MMP signaling axis was involved in the low UA-induced degradation of elastin, and that physiological concentrations of UA and p-Erk1/2-specific inhibitor exerted a protective role against elastin damage.

Taken together, the data presented here confirmed that low SUA levels exacerbated ICH by increasing the activity of the Erk1/2-MMP axis, thereby disrupting the integrity of the cerebrovascular.

Discussion

ICH is responsible for significant morbidity and mortality in adults. Hence, there is a need to increase the focus on improving understanding of the mechanisms and pathology of this condition. In the present study, we developed the first low UA model and proposed a possible mechanism by which low SUA could contribute to ICH pathogenesis. Our data show that low SUA levels increased the risk of R-ICH and cardiac-cerebral vascular mortality in ICH patients over 60 years old. We showed for the first time that low UA levels increased the likelihood of developing ICH and promoted ICH progression in hypertensive mice. We have also proposed a molecular mechanism by which low SUA levels could contribute to ICH via the upregulation of Erk1/2-MMP axis activity, the degradation of elastin, and the disruption of SMC-elastin contractile units. Furthermore, we found that the p-Erk1/2-MMP signaling axis were involved in low UA-induced degradation of elastin, and that physiological concentrations of UA and a p-Erk1/2-specific inhibitor exerted a protective role against elastin damage.

Previous studies have suggested that hyperuricemia is associated with a higher risk of hypertension, CVD-related mortality, and stroke [5–7]. Most studies have not distinguished the mortality risks among different SUA strata or various stroke subtypes. The first large-scale cohort study found that low SUA levels independently predicted higher all-cause and CVD-related mortality in the elderly population, particularly those who are malnourished [21]. Gerber et al. found that stroke showed a U-shaped relationship with SUA in elderly people. Adjusting for confounders reduced the risk of the upper quintile but did not attenuate the association between low SUA levels and stroke, particularly in ICH [6]. While that study evaluated a small sample size of 46 hemorrhagic stroke patients, our study included a total of 3138 subjects, including 351 hypertensive ICH patients. In addition, our epidemiological results further indicated that low SUA levels increase the risk of R-ICH and cardiac-cerebral vascular mortality in ICH patients over 60 years old. Moreover, the plasma metabolomics of R-ICH and ICH patients indicated that UA levels are significantly lower in the R-ICH group than in the ICH group. Our data confirmed the relationships between low SUA levels

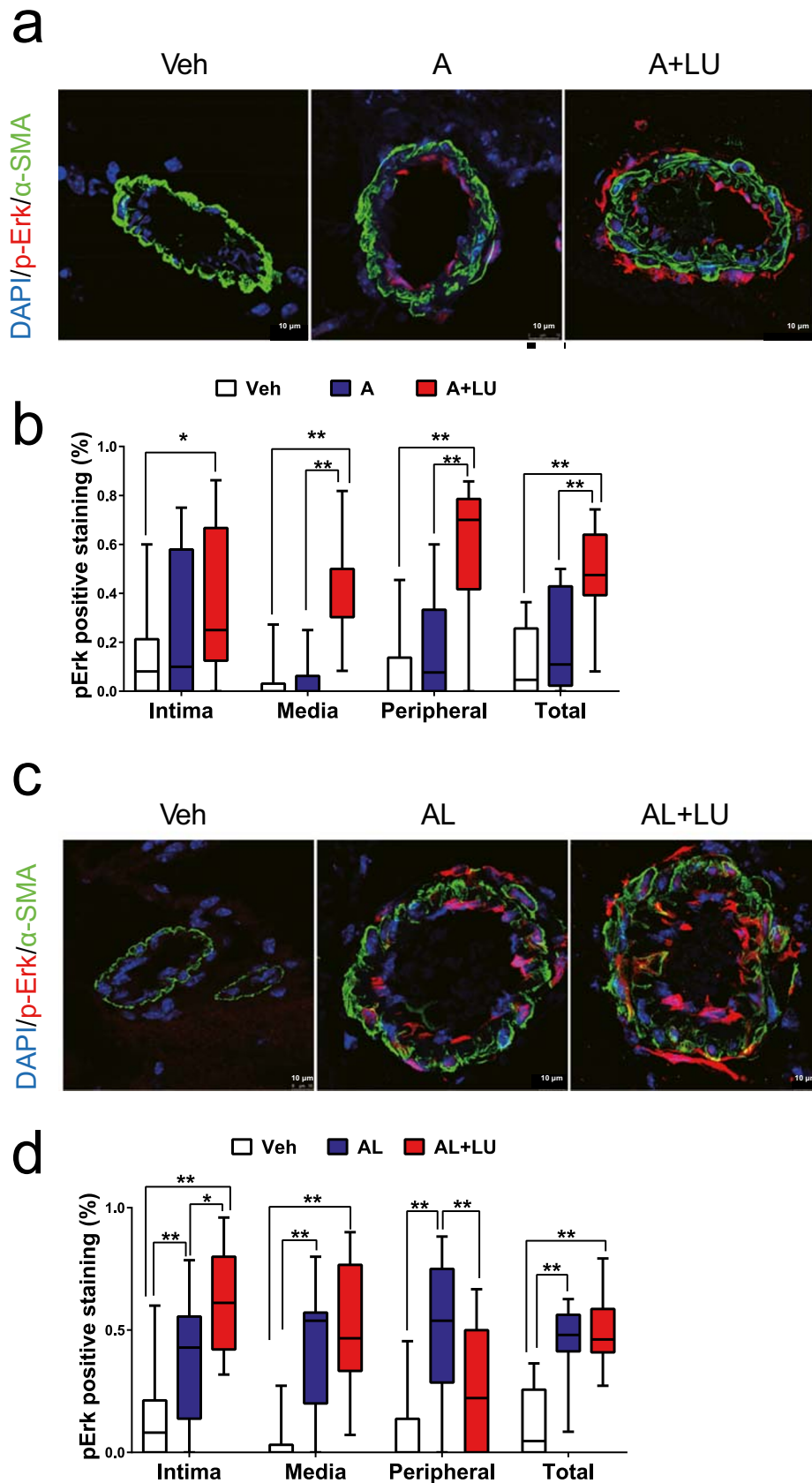


Fig. 6 Low uric acid increased Erk1/2 activity in ICH mice. **a, c** Representative images of p-Erk1/2 co-staining with α-SMA in the different groups. **b, d** Quantification of p-Erk1/2-positive cells in the cerebrovascular ($n = 5$). $*p < 0.05$, $**p < 0.01$. (Scales bar are shown in the image)

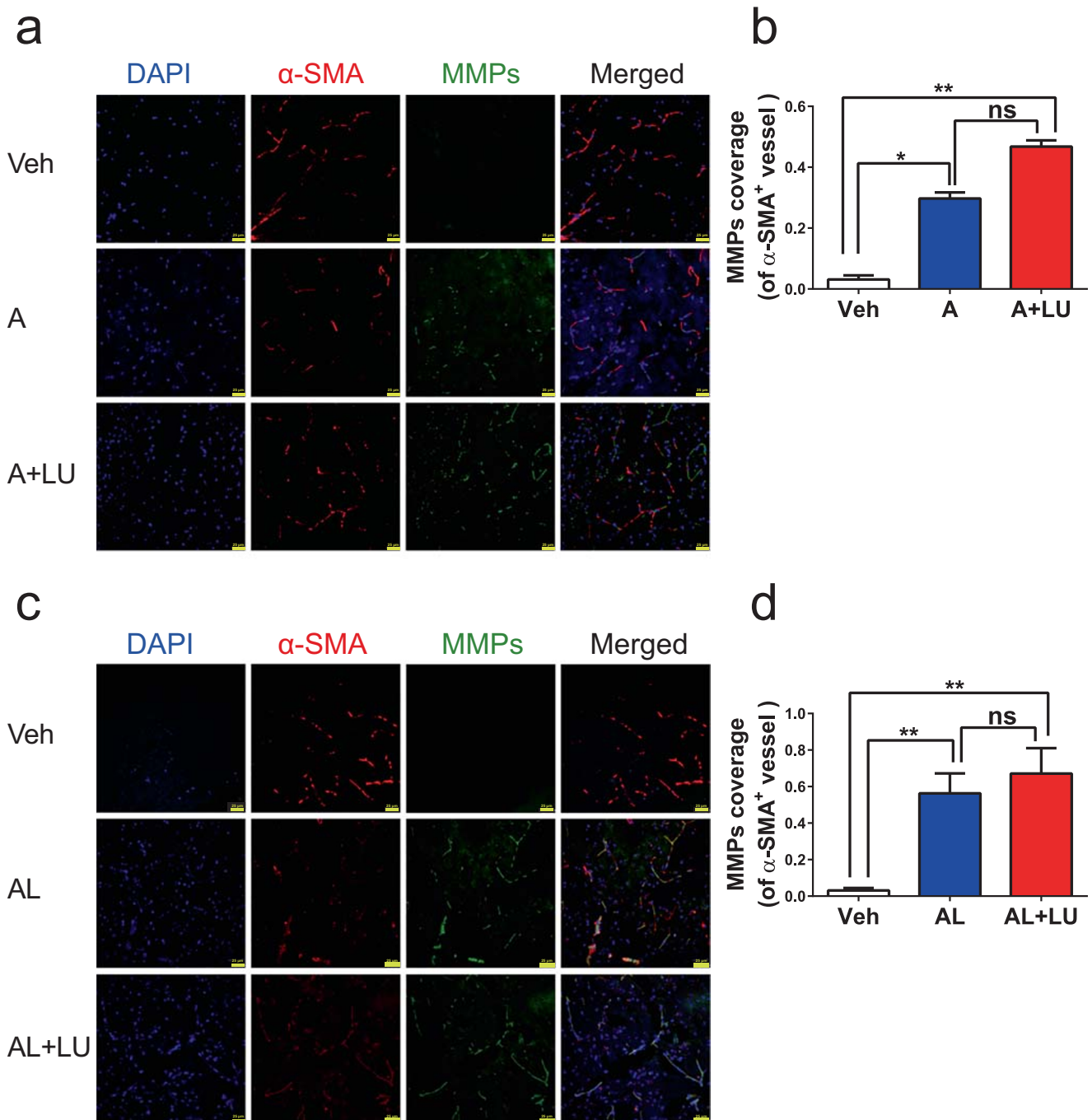


Fig. 7 Low uric acid increased MMPs activity in ICH mice. **a, c** Representative images of in situ MMPs activity in the brain sections from each group. **b, d** Quantification of MMPs coverage on α -SMA⁺ vessels ($n = 5$). * $p < 0.05$, ** $p < 0.01$, ns, not significant. (Scales bar are shown in the image)

and ICH and indicated that low SUA levels are new important risk factor for ICH.

Numerous studies have focused on brain damage and neuroprotection after ICH [22–24], although few have attempted to obtain an overall picture of the cerebrovascular alterations that cause ICH progression. Long noncoding RNA (lncRNA) and messenger RNA (mRNA) have been reported to be involved in post-ICH injury and repair [25]. Stroke-prone

spontaneous hypertensive rats (SHRSPs) usually developed ischemic stroke [26], while other researchers induced ICH by injecting collagenase or autologous blood into the brain [27–29]; however, neither of these animal models developed spontaneous ICH. Donald D and colleagues created several spontaneous ICH models in 8-month-old mice to study this mechanism [10–12] and found that increases in oxidative stress contributed to spontaneous ICH by activating MMP-9.

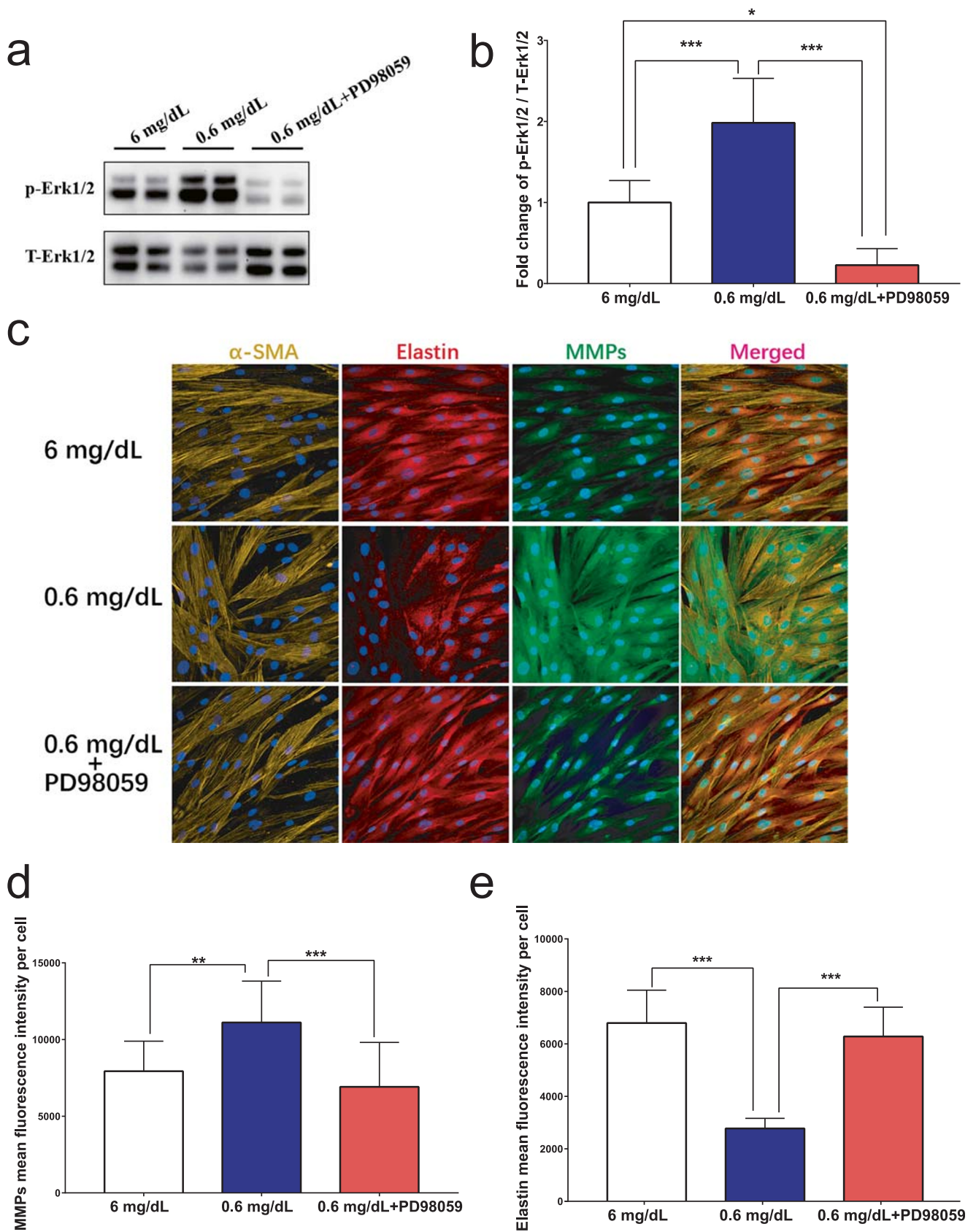


Fig. 8 Low concentration UA exposure increased phosphorylation of Erk1/2, MMPs activity and degraded elastin expression at 240 min after subjected to different co-culture conditions in vitro. **a, b** Western blot analysis of p-Erk1/2

in HBSMCs. **c** Representative images of MMPs, Elastin co-staining with α -SMA in the different co-culture conditions. **d, e** Quantification of MMPs and Elastin in different exposure. $n = 6$, $*p < 0.05$, $**p < 0.01$, $***p < 0.001$

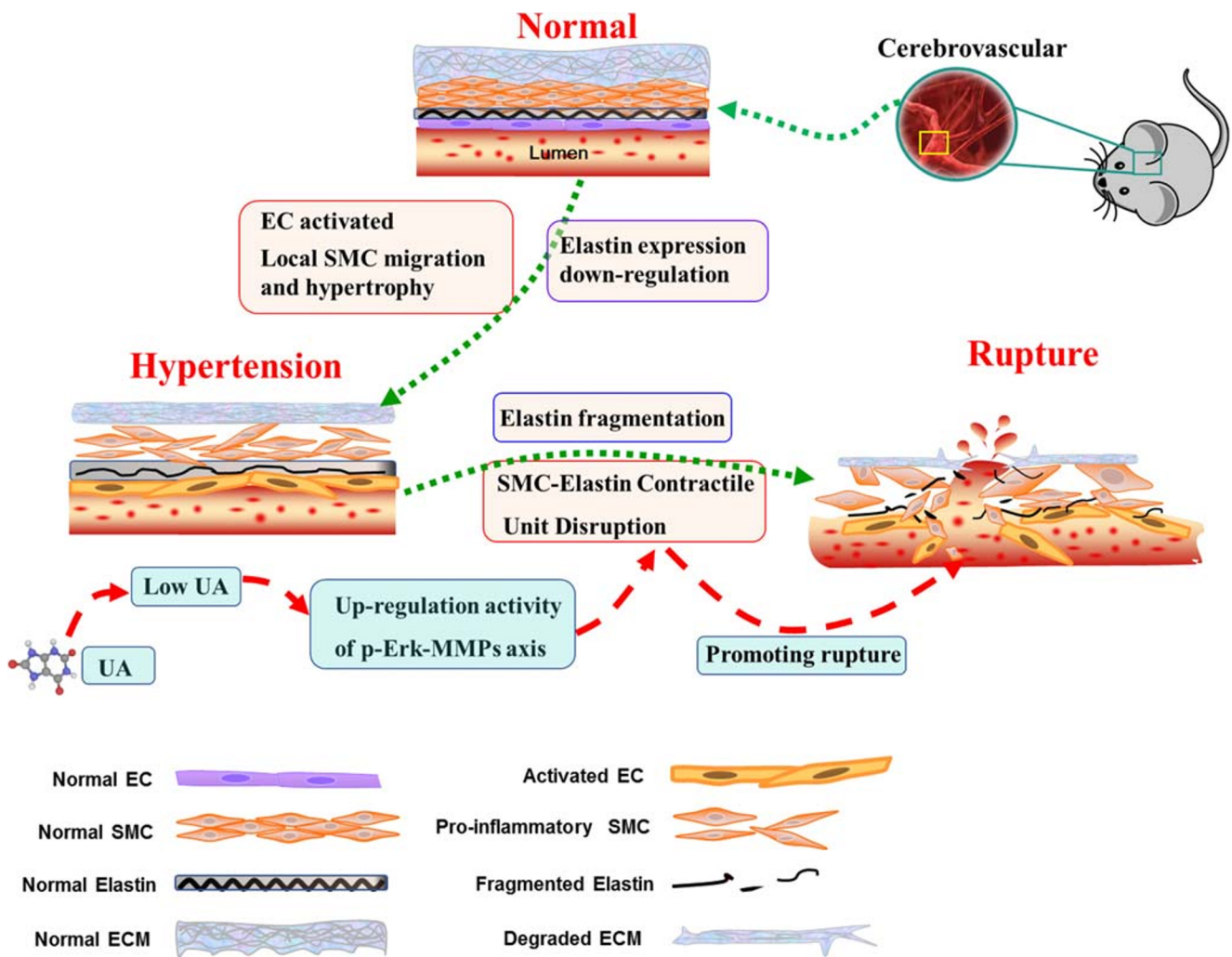


Fig. 9 Scheme of the possible mechanism by which low uric acid acts on ICH pathogenesis. The cerebrovascular components that presented alterations induced by hypertension were endothelial cell (EC) activation and dysfunction as well as local vascular smooth muscle cell (VSMC) migration and proliferation. The low SUA levels promoted

progressive damage in the cerebrovascular walls via disruption of the SMC-elastin contractile unit and upregulation of Erk1/2-MMPs activity, which degraded elastin and other components of the extracellular matrix (ECM) such as collagen. The further degeneration of the cerebrovascular structure ultimately led to vessel rupture

Similarly, Meissner et al. developed a cerebral small vessel disease (cSVD) model in 16-week-old mice [13]. However, this model was characterized by cerebrovascular alterations associated with a mild form of cognitive impairment and sporadic microbleeding. The most important reason for the difference among these phenotypes may be the ages of the mice because age has been shown to have a significant association with ICH [4]. With regard for age, Toth et al. used similar models and reported that aging exacerbates hypertension-induced cerebral hemorrhage in 24-month-old mice by increasing in oxidative stress and activation of MMPs [30]. The spontaneous ICH model described herein was established by modifying protocols [11]. We developed the first low UA mouse model by administering allopurinol and benzbromarone. Allopurinol, a xanthine oxidase (XO) inhibitor, yields other benefits in addition to potently reducing UA

levels. Allopurinol protects against western diet-induced vascular oxidative stress and aortic stiffness in females [31]. Moreover, allopurinol has been shown to reduce oxidative stress in the vasculature [32], improve endothelial function in CVD [33], decreased inflammatory indices [34], protected peripheral vascular function in ischemic stroke [35], and improved cerebrovascular endothelial function in diabetes [36]. Benzbromarone, a uricosuric drug, reduced arteriolar hyalinosis, interstitial fibrosis, and macrophage infiltration and protected renal function in a cyclosporine model [37]. Although we did not observe that allopurinol and benzbromarone exerted a direct protective effect, our histomorphology data indicated that the cerebrovascular was not negatively impacted in the low UA model. Based on that observation, we established low UA models with spontaneous ICH

without using Ang II bolus injections, unlike previously reported models [11].

The SMC-elastin contractile unit confers elasticity and strength to the vasculature and plays a vital role in the cerebrovascular. Disruption of the SMC-elastin contractile unit has been shown to be involved in the pathological processes of TAA and dissections (TAD) [38]. Disruption of the SMC-elastin contractile unit, elastin fragmentation, and vascular smooth muscle cell (VSMC) apoptosis has also been shown to contribute to intracranial aneurysm (IA), another vascular rupture-related disease [39]. Most IA models were induced by injecting elastase into the cerebrospinal fluid [40, 41]. In addition, elastase-induced fragmentation of the elastin lamina led to the successful development of carotid artery aneurysms and aortic aneurysms [40]. Here, we provide the first data indicating that elastin lamina is fragmented in ICH mice, similar to what has been observed in TAA. However, we have not observed cerebrovascular aneurysms in ICH mice. These cerebrovascular structure alterations of the SMC-elastin contractile unit might ultimately contribute to hypertension-induced cerebrovascular rupture.

To explore the mechanism by which low SUA levels contribute to ICH pathogenesis, we explored causal networks and hub genes with RNA-seq analysis. Unlike previous findings, we focused on cerebrovascular alterations in the pathogenesis of ICH. Then, we isolated the cerebrovasculature rather than whole-brain tissue for RNA-seq. Our data indicated that Erk1/2 plays a vital role in the pathogenesis of ICH. Fibulin-4 mutant mice have defects in elastic fiber assembly, which contributes to TAA rupture, and markedly upregulated levels of p-Erk1/2 in the aortic wall [42]. Previous studies have demonstrated that there is a close relationship between Erk1/2 and MMPs [43]. Yang et al. found that miconazole suppresses ICH by decreasing Erk1/2-MMP-9 signaling, and this shed light on the potential of new drug candidates for hemorrhagic stroke [14]. Our previous data showed that the levels of MMP-9 and MMP-2 activity were higher in ICH mice than in the vehicle group [44]. Yuan et al. found that Erk1/2 was also involved in the pathogenesis of ICH and that inhibiting Erk1/2 and p38 efficiently inhibited ICH-induced inflammatory damage [45]. Consistent with previous studies, our data also show that Erk1/2-MMP signaling is significantly increased in low SUA ICH mice. Col IV is the main component of the extracellular matrix (ECM) and is regulated by MMPs. Mutations in Col IV can lead to ICH in both humans and mice [46, 47]. MMPs degrade elastin and ECM, thereby disrupting the SMC-elastin contractile units and weakening the vascular structure. Our results reveal that low SUA levels exacerbate the pathological process of ICH via the upregulation of the Erk1/2-MMP axis. To further confirm the relationships between low UA levels, the p-Erk1/2-MMP axis, and elastin damage, we examined whether low UA (0.6 mg/dL) exposure would increase phosphorylation of Erk1/2 and MMP activity

and degrade elastin expression in HBSMCs. Our data demonstrate that low UA levels induced the activation of MMPs via Erk1/2 signaling pathway and partially inhibited by physiological concentrations of UA. This was confirmed by an effect of p-Erk1/2 phosphorylation inhibitor, PD98059, which decreased low UA-induced MMP activity, in part by dephosphorylation of Erk1/2. Similar to our results, Lai et al. reported that physiological concentrations of UA displayed anti-inflammatory and chondroprotective effects via the Erk1/2 signaling pathway and inhibited the activation of MMP [48]. At pathologically high levels (100 mM), homocysteine-induced oxidative stress led to activation of MMP-9 via the Erk-1/2 signaling pathway, and effect that can be decreased by UA in mouse brain endothelial cells [49]. DiCamillo et al. reported that neutrophil elastase (NE), when applied at low physiological concentrations, decreased tropoelastin (precursor molecules of elastin) mRNA expression by activating Erk1/2 in fibroblasts. Pretreatment with PD98059 abrogated the NE-initiated tropoelastin mRNA suppression [50].

These findings implicate p-Erk1/2-MMP signaling axis involved in the low UA level-induced degradation of elastin and show that physiological concentrations of UA and p-Erk1/2-specific inhibitor exerted a protective role against elastin damage.

Based on this study and previous work, we proposed that low SUA levels upregulated the activity of the Erk1/2-MMP axis and enhanced the degradation of elastin, collagen, and ECM, thereby disrupting SMC-elastin contractile units. Further inflammation and cerebrovascular structure degeneration ultimately lead to vessel rupture (Fig. 9).

In conclusion, this is the first study to confirm the relationship between low SUA levels and ICH and the first report to demonstrate a possible mechanism by which low SUA levels could promote ICH. A better understanding of ICH pathogenesis is important for the successful prevention of ICH progression and recurrence. Our data may shed light on ICH prevention and therapy.

Funding Information This work was supported by grants from the National Natural Science Foundations of China (81670386 and 91539113), CAMS Innovation Fund for Medical Sciences (CAMS-I2M, 2016-I2M-1-015), and the National Basic Research Program of China (973 Program, 2014CB541601 to JC).

Compliance with Ethical Standards

Conflict of Interest The authors declare that they have no conflict of interest.

Ethical Approval This study approved by the Human Ethics Committee, Fuwai Hospital (Approval No.: 2016-732). Patients or their caregivers provided informed consent. Animal experiments granted by the Animal Ethics Committee, Fuwai Hospital (Approval No.: 0085-M-200-HX).

References

- Qureshi AI, Mendelow AD, Hanley DF. Intracerebral haemorrhage. *Lancet*. 2009;373(9675):1632–44. [https://doi.org/10.1016/S0140-6736\(09\)60371-8](https://doi.org/10.1016/S0140-6736(09)60371-8).
- Ariesen MJ, Claus SP, Rinkel GJ, Algra A. Risk factors for intracerebral hemorrhage in the general population: a systematic review. *Stroke*. 2003;34(8):2060–5. <https://doi.org/10.1161/01.STR.0000080678.09344.8D>.
- Wang W, Jiang B, Sun H, Ru X, Sun D, Wang L, et al. Prevalence, incidence, and mortality of stroke in China: results from a nationwide population-based survey of 480 687 adults. *Circulation*. 2017;135(8):759–71. <https://doi.org/10.1161/CIRCULATIONAHA.116.025250>.
- Zia E, Hedblad B, Pessah-Rasmussen H, Berglund G, Janzon L, Engstrom G. Blood pressure in relation to the incidence of cerebral infarction and intracerebral hemorrhage. Hypertensive hemorrhage: debated nomenclature is still relevant. *Stroke*. 2007;38(10):2681–5. <https://doi.org/10.1161/STROKEAHA.106.479725>.
- Feig DI, Kang DH, Johnson RJ. Uric acid and cardiovascular risk. *N Engl J Med*. 2008;359(17):1811–21. <https://doi.org/10.1056/NEJMr0800885>.
- Gerber Y, Tanne D, Medalie JH, Goldbourt U. Serum uric acid and long-term mortality from stroke, coronary heart disease and all causes. *Eur J Cardiovasc Prev Rehabil*. 2006;13(2):193–8. <https://doi.org/10.1097/01.hjr.0000192745.26973.00>.
- Gu J, Fan YQ, Zhang HL, Zhang JF, Wang CQ. Serum uric acid is associated with incidence of heart failure with preserved ejection fraction and cardiovascular events in patients with arterial hypertension. *J Clin Hypertens*. 2018;20(3):560–7. <https://doi.org/10.1111/jch.13210>.
- Norvik JV, Schirmer H, Ytrehus K, Storhaug HM, Jenssen TG, Eriksen BO, et al. Uric acid predicts mortality and ischaemic stroke in subjects with diastolic dysfunction: the Tromso Study 1994–2013. *ESC Heart Fail*. 2017;4(2):154–61. <https://doi.org/10.1002/ehf2.12134>.
- Anand NN, Padma V, Prasad A, Alam KC, Javid MS. Serum uric acid in new and recent onset primary hypertension. *J Pharm Bioall Sci*. 2015;7(Suppl 1):S4–8. <https://doi.org/10.4103/0975-7406.155763>.
- Iida S, Baumbach GL, Lavoie JL, Faraci FM, Sigmund CD, Heistad DD. Spontaneous stroke in a genetic model of hypertension in mice. *Stroke*. 2005;36(6):1253–8. <https://doi.org/10.1161/01.str.0000167694.58419.a2>.
- Wakisaka Y, Chu Y, Miller JD, Rosenberg GA, Heistad DD. Spontaneous intracerebral hemorrhage during acute and chronic hypertension in mice. *J Cereb Blood Flow Metab*. 2010;30(1):56–69. <https://doi.org/10.1038/jcbfm.2009.183>.
- Wakisaka Y, Chu Y, Miller JD, Rosenberg GA, Heistad DD. Critical role for copper/zinc-superoxide dismutase in preventing spontaneous intracerebral hemorrhage during acute and chronic hypertension in mice. *Stroke*. 2010;41(4):790.
- Meissner A, Minnerup J, Soria G, Planas AM. Structural and functional brain alterations in a murine model of angiotensin II-induced hypertension. *J Neurochem*. 2017;140(3):509–21. <https://doi.org/10.1111/jnc.13905>.
- Yang R, Zhang Y, Huang D, Luo X, Zhang L, Zhu X, et al. Miconazole protects blood vessels from MMP9-dependent rupture and hemorrhage. *Dis Model Mech*. 2017;10(3):337–48. <https://doi.org/10.1242/dmm.027268>.
- Li Z, Sun L, Zhang H, Liao Y, Wang D, Zhao B, et al. Elevated plasma homocysteine was associated with hemorrhagic and ischemic stroke, but methylenetetrahydrofolate reductase gene C677T polymorphism was a risk factor for thrombotic stroke: a Multicenter Case-Control Study in China. *Stroke*. 2003;34(9):2085.
- Yamakawa H, Jezova M, Ando H, Saavedra JM. Normalization of endothelial and inducible nitric oxide synthase expression in brain microvessels of spontaneously hypertensive rats by angiotensin II AT1 receptor inhibition. *J Cereb Blood Flow Metab*. 2003;23(3):371.
- Bengrine A, Da SC, Massy ZA, Boullier A, Bugnicourt JM, Chillon JM. Cerebral arterioles preparation and PECAM-1 expression in C57BL/6J and ApoE^{-/-} mice. *Front Biosci*. 2011;16(2):2367.
- Helske S, Syvaranta S, Kupari M, Lappalainen J, Laine M, Lommi J, et al. Possible role for mast cell-derived cathepsin G in the adverse remodelling of stenotic aortic valves. *Eur Heart J*. 2006;27(12):1495–504. <https://doi.org/10.1093/eurheartj/ehi706>.
- Krishna SM, Seto SW, Jose RJ, Biros E, Moran CS, Wang Y, et al. A peptide antagonist of thrombospondin-1 promotes abdominal aortic aneurysm progression in the angiotensin II-infused apolipoprotein-E-deficient mouse. *Arterioscler Thromb Vasc Biol*. 2015;35(2):389–98. <https://doi.org/10.1161/ATVBAHA.114.304732>.
- Yuan F, Wang Y, Guan Y, Ren Y, Lu H, Xiao T, et al. Real-time imaging of mouse lenticulostriate artery following brain ischemia. *Front Biosci (Elite Ed)*. 2013;5:517–24. <https://doi.org/10.2741/e633>.
- Tseng WC, Chen YT, Ou SM, Shih CJ, Tamg DC, Taiwan Geriatric Kidney Disease Research G. U-shaped association between serum uric acid levels with cardiovascular and all-cause mortality in the elderly: the role of malnourishment. *J Am Heart Assoc*. 2018;7(4). <https://doi.org/10.1161/JAHA.117.007523>.
- Zhou L, Liu C, Wang Z, Shen H, Wen Z, Chen D, et al. Pannexin-1 is involved in neuronal apoptosis and degeneration in experimental intracerebral hemorrhage in rats. *Mol Med Rep*. 2018;17(4):5684–91. <https://doi.org/10.3892/mmr.2018.8624>.
- Han X, Zhao X, Lan X, Li Q, Gao Y, Liu X, et al. 20-HETE synthesis inhibition promotes cerebral protection after intracerebral hemorrhage without inhibiting angiogenesis. *J Cereb Blood Flow Metab*. 2018. <https://doi.org/10.1177/0271678X18762645>.
- Zhou Y, Wang S, Li Y, Yu S, Zhao Y. SIRT1/PGC-1 α signaling promotes mitochondrial functional recovery and reduces apoptosis after intracerebral hemorrhage in rats. *Front Mol Neurosci*. 2017;10:443. <https://doi.org/10.3389/fnmol.2017.00443>.
- Hanjin C, Tao L, Pengfei L, Ali Y, Huajun Z, Jiekun L, et al. Altered long noncoding RNA and messenger RNA expression in experimental intracerebral hemorrhage—a preliminary study. *Cell Physiol Biochem*. 2018;45(3):1284–301. <https://doi.org/10.1159/000487464>.
- Sadoshima S, Busija D, Brody M, Heistad D. Sympathetic nerves protect against stroke in stroke-prone hypertensive rats. A preliminary report. *Hypertension*. 1981;3(3 Pt 2):I124–7.
- MacLellan CL, Silasi G, Poon CC, Edmundson CL, Buist R, Peeling J, et al. Intracerebral hemorrhage models in rat: comparing collagenase to blood infusion. *J Cereb Blood Flow Metab*. 2008;28(3):516–25. <https://doi.org/10.1038/sj.jcbfm.9600548>.
- Hsieh JT, Lei B, Sheng H, Venkatraman T, Lascola CD, Warner DS, et al. Sex-specific effects of progesterone on early outcome of intracerebral hemorrhage. *Neuroendocrinology*. 2016;103(5):518–30. <https://doi.org/10.1159/000440883>.
- Cao S, Hua Y, Keep RF, Chaudhary N, Xi G. Minocycline effects on intracerebral hemorrhage-induced iron overload in aged rats: brain iron quantification with magnetic resonance imaging. *Stroke*. 2018. <https://doi.org/10.1161/STROKEAHA.117.019860>.
- Toth P, Tarantini S, Springo Z, Tucsek Z, Gautam T, Giles CB, et al. Aging exacerbates hypertension-induced cerebral microhemorrhages in mice: role of resveratrol treatment in vasoprotection. *Aging Cell*. 2015;14(3):400–8. <https://doi.org/10.1111/acel.12315>.
- Lastra G, Manrique C, Jia G, Aroor AR, Hayden MR, Barron BJ, et al. Xanthine oxidase inhibition protects against Western diet-

- induced aortic stiffness and impaired vasorelaxation in female mice. *Am J Physiol Regul Integr Comp Physiol*. 2017;313(2):R67–77. <https://doi.org/10.1152/ajpregu.00483.2016>.
32. Berry C, Hamilton CA, Brosnan MJ, Magill FG, Berg GA, McMurray JJV, et al. Investigation into the sources of superoxide in human blood vessels angiotensin II increases superoxide production in human internal mammary arteries. *Circulation*. 2000;101(18):2206.
 33. Dawson J, Quinn T, Walters M. Uric acid reduction: a new paradigm in the management of cardiovascular risk? *Curr Med Chem*. 2007;14(17).
 34. Muir SW, Harrow C, Dawson J, Lees KR, Weir CJ, Sattar N, et al. Allopurinol use yields potentially beneficial effects on inflammatory indices in those with recent ischemic stroke: a randomized, double-blind, placebo-controlled trial. *Stroke*. 2008;39(12):3303–7.
 35. Khan F, George J, Wong K, Mcswiggan S, Struthers AD, Belch JJ. Allopurinol treatment reduces arterial wave reflection in stroke survivors. *Cardiovasc Ther*. 2008;26(4):247–52.
 36. Dawson J, Quinn TC, Lees K, Weir C, Cleland S, Walters M. Allopurinol and nitric oxide activity in the cerebral circulation of those with diabetes: a randomized trial. *Diabetes Care*. 2009;32(1):135–7.
 37. Mazali FC, Johnson RJ, Mazzali M. Use of uric acid-lowering agents limits experimental cyclosporine nephropathy. *Nephron Exp Nephrol*. 2011;120(1):12–9.
 38. Yamashiro Y, Yanagisawa H. Crossing bridges between extra- and intra-cellular events in thoracic aortic aneurysms. *J Atheroscler Thromb*. 2018;25(2):99–110. <https://doi.org/10.5551/jat.RV17015>.
 39. Chalouhi N, Hoh BL, Hasan D. Review of cerebral aneurysm formation, growth, and rupture. *Stroke*. 2013;44(12):3613–22. <https://doi.org/10.1161/STROKEAHA.113.002390>.
 40. Nuki Y, Tsou TL, Kurihara C, Kanematsu M, Kanematsu Y, Hashimoto T. Elastase-induced intracranial aneurysms in hypertensive mice. *Hypertension*. 2009;54(6):1337–44. <https://doi.org/10.1161/HYPERTENSIONAHA.109.138297>.
 41. Hosaka K, Downes DP, Nowicki KW, Hoh BL. Modified murine intracranial aneurysm model: aneurysm formation and rupture by elastase and hypertension. *J Neurointerv Surg*. 2014;6(6):474–9. <https://doi.org/10.1136/neurintsurg-2013-010788>.
 42. Huang J, Davis EC, Chapman SL, Budatha M, Marmorstein LY, Word RA, et al. Fibulin-4 deficiency results in ascending aortic aneurysms: a potential link between abnormal smooth muscle cell phenotype and aneurysm progression. *Circ Res*. 2010;106(3):583–92. <https://doi.org/10.1161/CIRCRESAHA.109.207852>.
 43. Garavello W, Maggioni D, Nicolini G, Motta L, Tredici G, Gaini R. Association between metalloproteinases 2 and 9 activity and ERK1/2 phosphorylation status in head and neck cancers: an ex vivo study. *Oncol Rep*. 2010;24(4):1073–8.
 44. Li H, Xu H, Wen H, Liu T, Sun Y, Xiao N, et al. Overexpression of LH3 reduces the incidence of hypertensive intracerebral hemorrhage in mice. *J Cereb Blood Flow Metab*. 2019;39(3):547–61. <https://doi.org/10.1177/0271678X18815791>.
 45. Yuan B, Fu F, Huang S, Lin C, Yang G, Ma K, et al. C5a/C5aR pathway plays a vital role in brain inflammatory injury via initiating Fgl-2 in intracerebral hemorrhage. *Mol Neurobiol*. 2017;54(8):6187–97.
 46. Gould DB, Phalan FC, Breedveld GJ, van Mil SE, Smith RS, Schimenti JC, et al. Mutations in Col4a1 cause perinatal cerebral hemorrhage and porencephaly. *Science*. 2005;308(5725):1167–71.
 47. Gould DB, Phalan FC, van Mil SE, Sundberg JP, Vahedi K, Massin P, et al. Role of COL4A1 in small-vessel disease and hemorrhagic stroke. *N Engl J Med*. 2006;354(14):1489–96. <https://doi.org/10.1056/NEJMoa053727>.
 48. Lai JH, Luo SF, Hung LF, Huang CY, Lien SB, Lin LC, et al. Physiological concentrations of soluble uric acid are chondroprotective and anti-inflammatory. *Sci Rep*. 2017;7(1):2359–12. <https://doi.org/10.1038/s41598-017-02640-0>.
 49. Tyagi N, Gillespie W, Vacek JC, Sen U, Tyagi SC, Lominadze D. Activation of GABA-A receptor ameliorates homocysteine-induced MMP-9 activation by ERK pathway. *J Cell Physiol*. 2009;220(1):257–66. <https://doi.org/10.1002/jcp.21757>.
 50. DiCamillo SJ, Carreras I, Panchenko MV, Stone PJ, Nugent MA, Foster JA, et al. Elastase-released epidermal growth factor recruits epidermal growth factor receptor and extracellular signal-regulated kinases to down-regulate tropoelastin mRNA in lung fibroblasts. *J Biol Chem*. 2002;277(21):18938–46. <https://doi.org/10.1074/jbc.M200243200>.

Publisher's Note Springer Nature remains neutral with regard to jurisdictional claims in published maps and institutional affiliations.